JOURNAL OF APPLIED ELECTROCHEMISTRY 21 (1991) 863–868

Synthesis of InSb and $In_xGa_{1-x}Sb$ thin films from electrodeposited elemental layers*

G. MENGOLI, M. M. MUSIANI, F. PAOLUCCI

Istituto di Polarografia ed Elettrochimica Preparativa del CNR, Corso Stati Uniti 4, 35020 Camin, Padova, Italy

M. GAZZANO

Centro di Studio per la Fisica delle Macromolecole del CNR, via Selmi 2, 40126 Bologna, Italy

Received 11 December 1990; revised 18 February 1991

The synthesis of thin films of indium and indium-gallium antimonides was performed by a method involving electrodeposition steps and thermal annealing. Successive layers of the elements were deposited in the order Sb, In and, when necessary, Ga. The binary InSb compound was obtained when annealing was performed at temperatures slightly higher than the In melting point. Ternary $In_xGa_{1-x}Sb$ films were also prepared by a similar method. These were found to consist of a single phase for $x \geqslant 0.91$ and of two phases, one rich in In and the other in Ga, for $x \leqslant 0.84$. The cubic lattice parameter was determined for all phases and used for calculating their composition, assuming Vegard's law as valid.

1. Introduction

Many successful electrochemical syntheses of semiconductor thin films have been described in recent years. These syntheses may or may not include non-electrochemical steps aimed at modifying either the chemical composition or the physical properties of the deposits. Both elemental and compound semiconductors may be achieved: while the former, Si [1, 2] and Ge [3], can be deposited only from fused salts or non-aqueous solvents, various II–VI and, to a lesser extent, III–V compound semiconductors are accessible from aqueous electrolytes. One remarkable achievement of the electrochemical methods is the preparation of polycrystalline thin films of materials of considerable molecular complexity such as ternary Cd chalcogenides ($CdSe_xTe_{1-x}$ [4–8], CdS_xSe_{1-x} [9]) or Cu–In chalcogenides ($CuInS_2$ [10], $CuInSe_2$ [11–15]). Under favourable experimental conditions both their chemical purity and physical properties are satisfactory. Thus, for instance, $CuInSe_2$ was directly obtained in crystalline form by electrolysis, with no need for thermal annealing [14, 15] and the purity of electrochemical $CdSe_{0.5}Te_{0.5}$ was good enough to allow its use in solar cells [7].

In contrast with II–VI compounds, ternary III–V semiconductors have so far not been synthesized by electrochemical means, in spite of their interest as mid-infrared detectors. For instance, advanced optoelectronic devices employ radiations of wavelength $\approx 2.5\,\mu m$ [16]. These devices imply the use of both sources and detectors made of semiconductors with an energy gap $\approx 0.5\,eV$, a value which falls in the range covered by Ga–In antimonides as well as Ga–In–As–Sb compounds [17, 18]. In principle, these materials do not need to be in the form of single large crystals but may be used as polycrystalline films 1–2 μm thick.

We have recently proposed a method for the preparation of GaSb [19], involving sequential deposition of Sb and Ga layers and thermal annealing of the two-layer deposit to yield a polycrystalline film. Although this method is less straightforward than cathodic codeposition, it has the advantage of being insensitive to large differences in the deposition potentials of the elements forming the compound semiconductor. Furthermore, each element may be deposited under appropriate conditions without any need for compromise between diverging requirements, and control of the stoichiometry is fairly easily achieved once deposition efficiencies are known. In the present paper attempts are described at extending the same method to InSb and ternary Ga–In–Sb compounds.

2. Experimental details

2.1. *Chemicals, substrates and electrodes*

$GaCl_3$ (99.99%, Aldrich), $InCl_3$ (ultrapure, Johnson Matthey), $SbCl_3$ (p.a., Merck), InSb (99.99%, Johnson Matthey), GaSb (99.9999%, Johnson Matthey) and all other chemicals were commercially available and used without any further purification.

Nickel plated (100 nm) copper sheets, prepared as previously described [19], were chosen as substrates for the preparation of the films. For stripping analysis, platinum sheets (1 cm^2) and an Sb disc (99.998%, Johnson Matthey, 0.33 cm^2) were used as working electrodes. An InSb electrode was also made from a small sample of the commercial polycrystalline compound.

* The paper is dedicated to Professor Dr Fritz Beck on the occasion of his 60th birthday.

0021-891X/91 $03.00 + .12

2.2. *Cells and equipment*

All electrochemical experiments were carried out in a glass cell having the working electrode and either a platinum spiral or platinum gauze used as counter-electrode in the same compartment. A saturated calomel reference electrode (SCE), to which all potentials are referred, was located in a separate compartment connected with the main one through a Luggin capillary. A computer-driven Solartron-Schlumberger 1286 Electrochemical Interface, a Hewlett-Packard ColorPro digital plotter and an AMEL Mod. 731 digital coulometer were used for electrochemical experiments. X-ray diffraction data were obtained with a Philips PW 1050/81 diffractometer controlled by a PW 1710 unit. The Ni-filtered CuK_α radiation (λ = 0.154 18 nm, 40 kV, 40 mA) was used. A 2θ range between 20 and 80 degrees was explored. The lattice parameter 'a' of the cell was determined by least squares refinements using the 8 most intense reflections. Crystallite size was estimated according to the Scherrer relation:

$$D = \lambda/\delta 2\theta \cos\theta$$

where λ is the X-ray wavelength, θ the Bragg angle and $\delta 2\theta$ the width of the reflection. A Warren's correction for instrumental line broadening was included. Secondary ion mass spectrometry (SIMS), scanning electron microscopy (SEM) and X-ray energy dispersive analysis (EDAX) measurements were obtained as described elsewhere [19]. Annealing treatments were carried out under dry nitrogen in a Pyrex-glass furnace connected to a vacuum-nitrogen line, heated by a heating muff whose temperature was fixed within 2° C of the desired value. Heating and cooling rates were 10–15° C min^{-1}.

2.3. *Electrodeposition baths and deposition procedures*

Antimony was deposited from 0.6 M $SbCl_3$, 1.6 M H_2SO_4, 1.7 M HCl [19, 20]. Indium was potentiostatically deposited from a chloride bath containing 0.3 M $InCl_3$ and 1 M KCl at −0.85 V (pH was adjusted to 1.5–2.0 with HCl). Gallium was potentiostatically deposited at −2.00 V from a 0.6 M $GaCl_3$ + 5 M KOH solution. All Sb and In depositions were carried out under stirring, at room temperature, while Ga deposition was carried out at 47° C

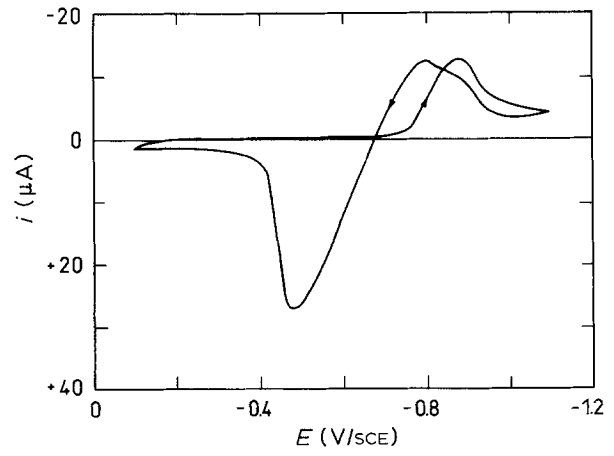

Fig. 1. Cyclic voltammetry obtained at a stationary Sb disc electrodes (0.2 cm^2) in a 0.3 M $InCl_3$ + 1 M KCl solution the pH of which was adjusted to 1.8 by HCl. Sweep rate 25 mV s^{-1}.

2.4. *Stripping voltammetry*

A strongly acidic stripping solution (1.7 M HCl, 1.6 M H_2SO_4) was used in order to avoid In passivation. Since in such a medium both Ni and Cu anodically dissolve at a potential slightly more positive than the dissolution potential of Sb, thus preventing accurate determination of the stripping charge of the latter, Pt was chosen as the substrate.

3. Results and discussion

3.1. *Preparation and characterization of InSb films*

Electrochemical synthesis of InSb by codeposition of the two elements from a citrate bath was first realized by Sadana and Singh [21] and then reproduced by Ortega and Herrero [22]. The preparation of InSb by sequential deposition of Sb and In followed by annealing was studied as both an alternative route to this compound and a preliminary step for the synthesis of ternary compounds.

Owing to the good stability of Sb in the electrolytic solution and at the potential used for In deposition, the sequence Sb first-In second was used.

The cyclic voltammetry in Fig. 1 shows the electrodeposition and stripping of In on an Sb disc electrode from the solution described in the experimental section. Except for the more marked hysteresis in the cathodic branch, it closely matches that obtained by Pletcher *et al.* on vitreous carbon [23]. Indium layers were potentiostatically deposited at E = −0.85 V on Sb films, obtained as in [19], with a 94% efficiency (by weighing). This value, which agrees with those observed on vitreous carbon, was taken into account in order to obtain the desired Sb/In ratio in the two-layer samples. These, either as-deposited or after annealing under nitrogen at various temperatures and for various times, were then characterized by linear stripping voltammetry and X-ray diffractometry.

Typical stripping voltammograms of In from an Sb substrate and of Sb from a Pt substrate (Fig. 2a), are compared with that recorded on an as-deposited two-layer sample ($\approx$2 μm overall thickness, Fig. 2b). The stripping peak at −0.63 V (Fig. 2a, solid line) is due to the anodic dissolution of the In deposit to In^{3+} [23, 24] (the formal potential for this process is $E°$ = −0.59 V/SCE [25]). The anodic peak at −0.021 V (Fig. 2a, dashed line) is attributed to dissolution of Sb as Sb^{3+} [26, 27]. The matching of stripping and deposition charges (allowance having been made for coulombic efficiency) confirms that passivation of neither metal occurs in this medium. The two peaks (at −0.64 and at −0.024 V, respectively) observed in the stripping voltammogram of the unannealed two-

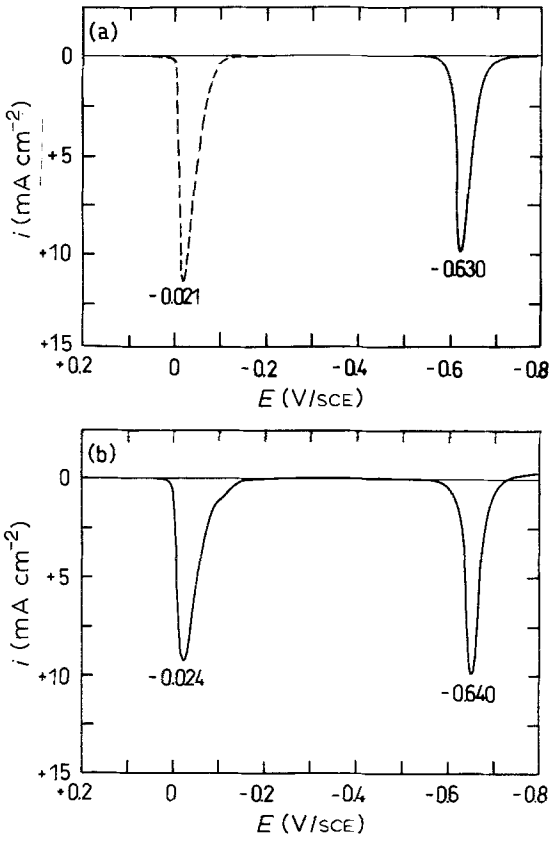

Fig. 2. (a) Stripping voltammograms of an In film deposited on Sb (solid line) and an Sb film deposited on Pt (dashed line), both in a 1.7 M HCl + 1.6 M H_2SO_4 solution. Sweep rate 1 mV s^{-1}. (b) Stripping voltammogram of an as-deposited two-layer sample consisting of an inner Sb and an outer In layer ($\approx 1\ \mu m$ each) deposited on a Pt substrate. Solution composition and sweep rate as for (a).

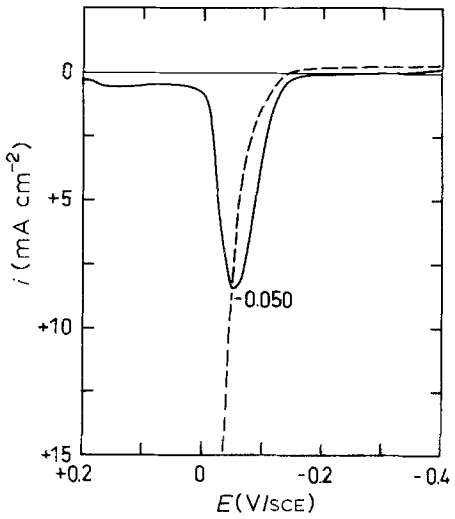

Fig. 3. Stripping voltammogram of a two-layer sample like that of Fig. 2b, after annealing at 185° C for 5 h (solid line) and anodic dissolution curve of an authentic InSb sample (dashed line). Stripping solution and sweep rate as for Fig. 2.

layer sample (Fig. 2b) almost coincide with those of Fig. 2a: the fact that the outermost layer is stripped first allows independent anodic dissolution of the two metals.

A slightly different stripping procedure was used for annealed samples since InSb may be converted to SbH_3 when polarized at potentials ≈ -0.6 V in acid medium, i.e. in the range where the In stripping peak occurs, while it is stable at $E = -0.3$ V. Therefore, linear voltammetries were performed by polarizing the electrode at -0.3 V and integrating the anodic current, if any, until it reached a negligible value, then sweeping the potential towards positive values. The anodic current flowing at -0.3 V was ascribed to dissolution of unreacted In. (The same precaution of avoiding potentials < -0.3 V appeared to be unnecessary for unannealed samples in which the In layer protected Sb from cathodic degradation [29]).

Stripping voltammetries recorded on a sample similar to that of Fig. 2b after annealing at 185° C for 5 h is shown in Fig. 3. In this instance, no charge attributable to unreacted In was observed; the charge recovered on the single anodic peak practically matched the sum of the deposition charges of both Sb and In. The potential region in which the annealed samples oxidize is consistent with the attribution of such a process to the anodic (six-electron) oxidation of InSb on the basis of comparison with literature data [30] and with our results on both InSb carbon-paste and InSb electrodes (Fig. 3, dashed line). The converted fraction of the deposited metals was calculated as $(Q_2 - Q_1)/(Q_2 + Q_1)$, where Q_1 is the charge flowing at $E = -0.3$ V (In) and Q_2 the charge associated to the peak at ≈ -0.025 V (a potential at which both Sb and InSb are oxidized [30]; compare Fig. 2 and 3). In any case, no weight loss due to annealing was found and the total charge recovered corresponded to the sum of the charges spent in the deposition of the components. The conversion data obtained under various annealing conditions are summarized in Table 1.

X-ray diffraction measurements were carried out on $\approx 6\ \mu m$ thick samples: only the reflections of the single components were detected after annealing treatment at 150° C, while both the characteristic reflections of InSb and those of unreacted In and Sb were present when annealing was carried out at 175° C, their relative amounts depending on annealing duration. Complete disappearance of the reflections of the components occurred by annealing at $\geqslant 185$° C for 5–10 h (Fig. 4, top half). The polycrystalline InSb phase was identified by comparison with JCPDS data [31] (see Table 2). The cubic lattice parameter was calculated to be 0.6463 ± 0.0004 nm. In all diffractometric spectra, the Cu and Ni reflections were detected, which ensured that the whole depth of the film was sampled.

Table 1. Conversion of two-layer In–Sb samples to InSb as a function of annealing conditions

T (° C)	Percent conversion after			
	1 h	2 h	5 h	15 h
150	–	–	–	0
175	67	69	78	87
185	87	–	99	–

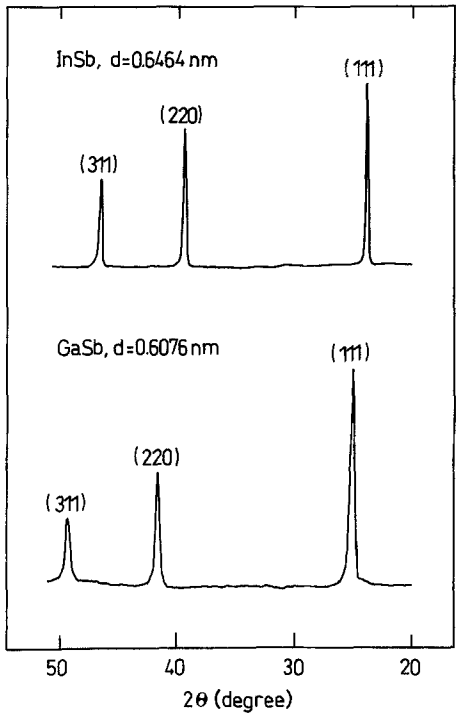

Fig. 4. X-ray diffraction patterns of electrochemically prepared InSb (top) and GaSb (bottom) thin films.

3.2. *Preparation and characterization of ternary In–Ga–Sb films*

Ga layers were deposited onto Sb–In two-layer samples for obtaining three-layer samples in which the amount of Ga + In (in moles) was equal to that of Sb. Cathodic deposition of Ga occurred on the In layer with an average current efficiency of 65%. (This value is markedly higher than that obtained when depositing Ga onto Sb [19]: a higher hydrogen evolution overpotential on In than on Sb, a more negative potential, a higher gallate concentration and a higher temperature [32] are all likely to improve the current efficiency of the process).

Stripping voltammetry of as-deposited samples showed that both Ga and In were stripped at the same potential, producing a single unresolved peak. The disappearance of this peak, used as a criterion for

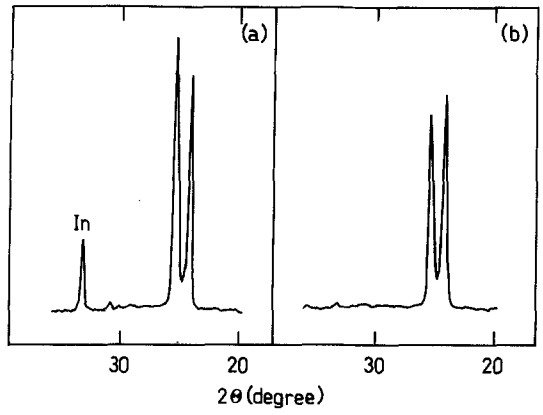

Fig. 5. Influence of annealing conditions on X-ray diffraction pattern of three-layer Sb-In-Ga samples: (a) 200° C for 12 h, (b) 400° C for 5 h.

Table 2. Comparison of experimental and JCPDS X-ray diffraction data for InSb

Experimental		*JCPDS*		
d (nm)	*Intensity*	*d (nm)*	*Intensity*	*hkl*
0.374	100	0.3740	100	111
0.229	75	0.2290	85	220
0.195	49	0.1953	55	311
0.162	13	0.1620	15	400
0.149	15	0.1486	22	331
0.132	21	0.1323	25	422
0.125	10	0.1247	12	511
0.115	6	0.1145	9	440

establishing the completeness of the thermally induced reaction was observed after 5 h heating at 400° C. Annealing conditions previously found suitable for inducing InSb formation (and, a fortiori, GaSb formation [19]) did not cause the disappearance of unreacted group III elements. X-ray diffraction experiments confirmed this picture. Figure 5 shows that annealing a three-layer sample at 200° C for 12 h left a fairly large amount of unreacted In (see peak at $2\theta = 33.2°$, corresponding to the $\langle 1\,1\,1\rangle$ reflection) and Sb (peak at $2\theta = 51.9°$, corresponding to the $\langle 0\,2\,2\rangle$ reflection, not shown in the figure) which were no longer found when an identical sample was kept at 400° C for 5 h (other features of the diffraction patterns in Fig. 5 will be discussed later).

Samples having variable ratios of In and Ga were investigated (their sum always corresponding to the Sb amount), all samples being annealed at 400° C for 5 h. Figure 6a shows the X-ray diffraction pattern obtained for a sample with an overall stoichiometry $In_{0.91}Ga_{0.09}Sb$. This pattern is very close to the InSb diffractogram and shows that the sample is isomorphous with it (compare Fig 4, top half) but with a smaller lattice parameter (0.6434 instead of 0.6464 nm, the difference being well above the experimental error of 0.0004 nm). Such a contraction of the lattice parameter is in agreement with the replacement of some of the In atoms by the smaller Ga. The cubic lattice dimension of a ternary compound $In_xGa_{1-x}Sb$ is related to the lattice parameters of binary compounds and mole fraction x through Vegard's law [33]:

$$a = a_{InSb}x + a_{GaSb}(1 - x)$$

provided that InSb and GaSb form a solid solution. If x is calculated from this equation, 0.92 ± 0.05 is obtained instead of 0.91. Table 3 shows that, for samples having $x \geqslant 0.91$, the expected monotonic decrease of the lattice parameter with increasing Ga content is observed.

X-ray diffraction patterns become more complex when Ga is present in larger relative amounts as shown in Fig. 6b for an overall composition $In_{0.8}Ga_{0.2}Sb$: the diffractogram appears as the sum of two contributions, one very similar to the InSb pattern and the other very similar to that of GaSb (the GaSb spectrum is reported in Fig. 4, bottom half). However, once again, the

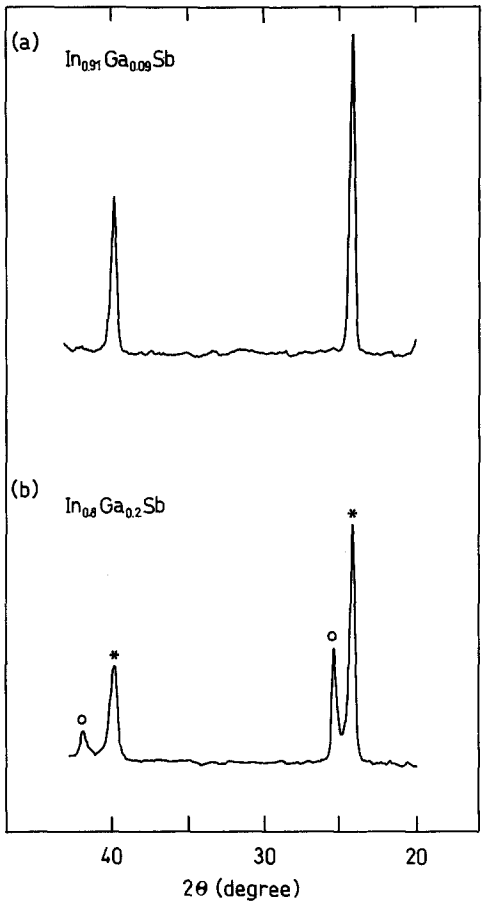

Fig. 6. X-ray diffraction patterns of electrochemically prepared ternary $In_xGa_{1-x}Sb$ samples. (a) $x = 0.91$, single phase; (b) $x = 0.8$, two-phase. (○) Ga-rich and (*) In-rich.

lattice parameters do not correspond to those of pure binary compounds. One is led to conclude that the sample consists of two ternary phases, one rich in In and the other in Ga. (The same peak attribution can be made for the sample in Fig. 5.) The lattice parameters measured for two-phase samples are reported in Table 3 as a function of overall composition. Vegard's law allows recalculation of the composition of each phase from the corresponding lattice parameter. Since the overall composition of each sample is known from electrochemical experiments, the percentage of, for example, the In-rich phase may easily be calculated as:

$$\%\text{In-rich phase} = \frac{x - x_{\text{Ga-rich}}}{x_{\text{In-rich}} - x_{\text{Ga-rich}}} \times 100$$

Table 3. Cubic lattice parameter of electrochemically prepared InSb, GaSb and $In_xGa_{1-x}Sb$

x*	*In-rich phase a (nm)*	*Ga-rich phase a (nm)*
1	0.6464 ± 0.0004	-
0.96	0.6454 ± 0.0004	-
0.91	0.6434 ± 0.0006	-
0.91	0.6438 ± 0.0006	-
0.79	0.6426 ± 0.0005	0.6092 ± 0.0005
0.70	0.6418 ± 0.0008	0.6104 ± 0.0005
0	-	0.6076 ± 0.0005

* Overall composition from electrochemical experiments

Table 4. Composition and relative amount of the two phases formed in $In_xGa_{1-x}Sb$ samples

Overall x	*x In-rich phase*	*(%)*	*x Ga-rich phase*	*(%)*
0.96	0.97	(100)	-	
0.91	0.93	(100)	-	
0.91	0.92	(100)	-	
0.84	0.93	(90)	0.02	(10)
0.79	0.90	(87)	0.04	(13)
0.79	0.89	(88)	0.03	(12)
0.78	0.86	(90)	0.08	(10)
0.70	0.88	(78)	0.07	(22)
0.67	0.86	(77)	0.04	(23)

where $x_{\text{In-rich}}$ and $x_{\text{Ga-rich}}$ are the stoichiometric indexes of In in the In-rich and Ga-rich phases respectively. These data, summarized in Table 4, show that: (i) for single-phase samples X-ray and electrochemical compositions are in good agreement; (ii) reproducibility is quite good; and (iii) for two-phase samples the composition of each phase is essentially independent of overall composition (maximum error on x is ≈ 0.05 for In-rich phases and ≈ 0.025 for Ga-rich phases; deviations from Vegard's law have previously been observed for the latter [34]).

The existence of a miscibility gap in the GaSb-InSb system was the object of some controversy in the 1950s–1960s [35–38]. Earlier reports of limited solid solubility [35, 36] were later criticized [37, 38]. More recently calculated phase diagrams do not indicate any miscibility gap at temperatures $\geqslant 400°$ C [39, 40], but do not rule out such a gap at room temperature. It is also known that $Ga_{1-x}In_xAs_ySb_{1-y}$ samples, the composition of which falls within the miscibility gap have been obtained in a metastable form [41]. It is shown in [40] that solidification of In–Ga–Sb solutions leads to continuous variation of the solid phase composition while solidification progresses (the extent of this variation is a function of temperature). This would imply continuous variation of the lattice parameter and, therefore broadening of the X-ray diffraction peaks. Thus, for example, instead of the two sharp ⟨1 1 1⟩ observed reflections, Fig. 6b, a single broad peak would be found.

Table 5 summarizes the crystallite size data of both binary and ternary films. When a range is reported, figures correspond to the minimum – maximum values measured on a series of samples. Previous reports on InSb electrodeposition [20, 21] contain no information on crystallite size, so that no comparison is pos-

Table 5. Average crystallite size of electrochemically prepared InSb, GaSb and $In_xGa_{1-x}Sb$ from X-ray data

Sample	*Crystallite size (nm)*
GaSb	60
InSb	35
Ga-rich phase in two-phase samples	28–88
In-rich phase in two-phase samples	20–49

sible. Crystallites of 20–200 nm size were also visible by SEM, which, however, showed larger features, up to a few micrometres, which may be interpreted as assembly of crystallites.

SIMS did not reveal any composition non-homogeneity along the direction perpendicular to the film. EDAX analysis, performed on various parts of ternary two-phase films by sampling a volume of 1–2 μm^3 each time, showed local stoichiometries clearly different from the average one. Both In- and Ga-rich areas were observed although, for the latter, a Ga amount as high as that shown in Table 4 for the Ga-rich phases was never obtained, since the sampled volume was much larger than the average crystallite volume.

4. Conclusion

The method previously proposed for the synthesis of GaSb films [19] has been extended to InSb and $In_xGa_{1-x}Sb$. While InSb films of comparable quality may be obtained by cathodic codeposition [21, 22], this is, to our knowledge, the first report of an electrochemically based synthesis of a ternary III–V compound.

X-ray characterization of the ternary films showed that only $In_xGa_{1-x}Sb$ samples with $x \geqslant 0.91$ form a single phase, while two phases were detected for lower x values. Comparison of this experimental result with literature data is not straightforward, since the latter refer to crystallization from an excess liquid phase while, for our system, a homogeneous liquid phase should not be attained at $\leqslant 400°C$: Ga and In melt during thermal annealing but no liquid In–Ga–Sb phase with an Sb atomic fraction 0.5 may exist at 400° C [34]. Therefore, compound formation is likely to occur through one or both of the following routes:

- progressive dissolution of Sb in the Ga–In solution and precipitation of antimonides from it, both at the annealing temperature and during exhaustive solidification of the melt;
- diffusion of III group metals into Sb and solid-phase reaction. This fairly complicated picture might be simplified by annealing at temperatures higher than 400° C which represent a present experimental limit.

References

[1] D. Elwell, R. S. Feigelson and G. M. Rao, *J. Electrochem. Soc.* **130** (1983) 1021.
[2] D. Elwell and G. M. Rao, *J. Appl. Electrochem.* **18** (1988) 15.
[3] W. Paatsch, *J. Electrochem. Soc.* **124** (1977) 1505.
[4] G. Hodes, *Nature* **285** (1980) 29.
[5] M. Skyllas-Kazacos, *J. Electroanal. Chem.* **148** (1983) 233.
[6] J. M. Rosamilla and B. Miller, *ibid.* **215** (1986) 249.
[7] R. N. Bhattacharya, *J. Appl. Electrochem.* **16** (1986) 168.
[8] Z. Loizos, N. Spyrellis, G. Maurin and D. Pottier, *J. Electroanal. Chem.* **269** (1989) 399.
[9] A. S. Baranski, W. R. Fawcett, K. Gatner, A. C. McDonald, J. R. MacDonald and M. Selen, *J. Electrochem. Soc.* **130** (1983) 579.
[10] R. Engelken, H. McCloud, E. Smith, D. Moss, H. Hormasji and N. Sanders, Committee Meeting of the Electrochemical Society, Atlanta (1988) Abstract No. 80.
[11] T. L. Chu, S. S. Chu, S. C. Lin and J. Yue, *J. Electrochem. Soc.* **131** (1984) 2182.
[12] G. Hodes, T. Engelhard, D. Cahen, L. L. Kazmerski and C. R. Herrington, *Thin Solid Films* **128** (1985) 93.
[13] C. D. Lokhande, *Bull. Electrochem.* **3** (1987) 219.
[14] D. Pottier and G. Maurin, *J. Appl. Electrochem.* **19** (1989) 361.
[15] D. Pottier, Doctoral Thesis. Paris, France (1990).
[16] B. Catania, *L'Elettrotecnica* **75** (1988) 13.
[17] N. Kobayashi, Y. Horikoshi and C. Uemura, *Jpn. J. Appl. Phys.* **19** (1980) L30.
[18] J. L. Zyskind, A. K. Srivastava, J. C. DeWinter, M. A. Pollack and J. W. Sulhoff, *J. Appl. Phys.* **61** (1987) 2898.
[19] F. Paolucci, G. Mengoli and M. M. Musiani, *J. Appl. Electrochem.* **20** (1990) 868.
[20] R. K. Iyer and S. G. Deshpande, *ibid.* **17** (1987) 936.
[21] Y. N. Sadana and J. P. Singh, *Plat. Surf. Finish.* **64** (1985) 64.
[22] J. Ortega and J. Herrero, *J. Electrochem. Soc.* **136** (1989) 3388.
[23] G. Gunawardena, D. Pletcher and A. Razaq, *J. Electroanal. Chem.* **164** (1984) 363.
[24] V. V. Losev and A. P. Pchelnikov, *Electrochim. Acta* **18** (1973) 589.
[25] M. Pourbaix, 'Atlas d'Equilibres Electrochimiques', Gauthier-Villars, Paris (1963), pp. 524 *ff.*
[26] I. A. Ammar and A. Saad *J. Electroanal. Chem.* **34** (1972) 159.
[27] L. L. Wikstrom, N. T. Thomas and K. Nobe, *J. Electrochem. Soc.* **122** (1975) 1201.
[28] A. S. Voevodskii, *Elektrokhim.* **10** (1974) 276.
[29] A. L. Pitman, M. Pourbaix and N. Zoubov, *J. Electrochem. Soc.* **104** (1957) 594.
[30] M. E. Straumanis and L. Hu, *J. Electrochem. Soc.* **119** (1972) 818.
[31] JCPDS file No. 6-0208.
[32] R. Dorin, E. J. Frazer, *J. Appl. Electrochem.* **18** (1988) 134.
[33] A. R. West, 'Solid State Chemistry and its Applications', John Wiley & Sons, Chichester, UK (1984) pp. 366 *ff.*
[34] J. C. Woolley and C. M. Gillet, *J. Phys. Chem. Solids* **17** (1960) 34.
[35] J. S. Blakemore, *Can. J. Phys.* **35** (1957) 35.
[36] C. Kolm, S. A. Kulin and B. L. Averbach, *Phys. Rev.* **108** (1957) 965.
[37] J. C. Woolley, B. A. Smith and D. G. Lees, *Proc. Phys. Soc., London* **72** (1958) 214.
[38] F. A. Trumbore, P. E. Freeland and A. D. Mills, *J. Electro-Chem. Soc.* **109** (1962) 645.
[39] G. M. Blom and T. S. Plaskett, *ibid.* **118** (1971) 1831.
[40] K. Onabe, *Jpn. J. Appl. Phys.* **21** (1982) 964.
[41] G. Bougnot, F. Delannay, A. Foucaran, F. Pascal, F. Roumanille, P. Grosse and J. Bougnot, *J. Electrochem. Soc.* **135** (1988) 1783.